



1 **Spring temperature variability over Turkey since 1800 CE reconstructed**
2 **from a broad network of tree-ring data**

3

4 **Nesibe Köse^{(1),*}, H. Tuncay Güner⁽¹⁾, Grant L. Harley⁽²⁾, Joel Guiot⁽³⁾**

5

6 ⁽¹⁾Istanbul University, Faculty of Forestry, Forest Botany Department 34473 Bahçeköy-Istanbul,
7 Turkey

8 ⁽²⁾University of Southern Mississippi, Department of Geography and Geology, 118 College
9 Drive Box 5051, Hattiesburg, Mississippi, 39406, USA

10 ⁽³⁾Aix-Marseille Université, CNRS, IRD, CEREGE UM34, ECCOREV, 13545 Aix-en-
11 Provence, France

12

13

14

15

16

17 *Corresponding author. Fax: +90 212 226 11 13

18 E-mail address: nesibe@istanbul.edu.tr

19



20 **Abstract**

21 The 20th century was marked by significant decreases in spring temperature ranges and increased
22 nighttime temperatures throughout Turkey. The meteorological observational period in Turkey,
23 which starts *ca.* 1929 CE, is too short for understanding long-term climatic variability. Hence,
24 the historical context of this gradual warming trend in spring temperatures is unclear. Here we
25 use a network of 23 tree-ring chronologies to provide a high-resolution spring (March–April)
26 temperature reconstruction over Turkey during the period 1800–2002. The reconstruction model
27 accounted for 67% (Adj. $R^2 = 0.64$, $p \leq 0.0001$) of the instrumental temperature variance over the
28 full calibration period (1930–2002). During the pre-instrumental period (1800–1929) we captured
29 more cold events ($n = 23$) than warm ($n = 13$), and extreme cold and warm events were typically
30 of short duration (1–2 years). Compared to coeval reconstructions of precipitation in the region,
31 our results are similar with durations of extreme wet and dry events. The reconstruction is
32 punctuated by a temperature increase during the 20th century; yet extreme cold and warm events
33 during the 19th century seem to eclipse conditions during the 20th century. During the 19th
34 century, annual temperature ranges are more volatile and characterized by more short-term
35 fluctuations compared to the 20th century. During the period 1900–2002, our reconstruction
36 shows a gradual warming trend, which includes the period during which diurnal temperature
37 ranges decreased as a result of increased urbanization in Turkey.

38

39 **KEYWORDS:** Dendroclimatology, Climate reconstruction, *Pinus nigra*, Principle component
40 analysis, Spring temperature.



41 **1 Introduction**

42

43 Significant decreases in spring diurnal temperature ranges (DTR) occurred throughout Turkey
44 from 1929 to 1999 (Turkes & Sumer 2004). This decrease in spring DTRs was characterized by
45 day-time temperatures that remained relatively constant while a significant increase in night-time
46 temperatures were recorded over western Turkey and were concentrated around urbanized and
47 rapidly-urbanizing cities. The historical context of this gradual warming trend in spring
48 temperatures is unclear as the high-quality meteorological records in Turkey, which start in
49 1929, are relatively short for understanding long-term climatic variability.

50

51 Tree rings have shown to provide useful information about the past climate of Turkey and were
52 used intensively during the last decade to reconstruct precipitation in the Aegean (Hughes et al.
53 2001, Griggs et al. 2007), Black Sea (Akkemik et al. 2005), Mediterranean regions (Touchan et
54 al. 2005a), as well as the Sivas (D'Arrigo & Cullen 2001), southwestern (Touchan et al. 2003,
55 Touchan et al. 2007), south-central (Akkemik & Aras 2005) and western Anatolian (Köse et al.
56 2011) regions of Turkey. These studies used tree rings to reconstruct precipitation because
57 available moisture is often found to be the most important limiting factor that influences radial
58 growth of many tree species in Turkey. These studies revealed past spring-summer precipitation,
59 and described past dry and wet events and their duration. Recently, Heinrich et al. (2013)
60 provided a winter-to-spring temperature proxy for Turkey from carbon isotopes within the
61 growth rings of *Juniperus excelsa* since AD 1125. Low-frequency temperature trends
62 corresponding to the Medieval Climatic Anomaly and Little Ice Age were identified in the
63 record, but the proxy failed to identify the recent warming trend during the 20th century. In this



64 study, we present a tree-ring based spring temperature reconstruction from Turkey and compare
65 our results to previous reconstructions of temperature and precipitation to provide a more
66 comprehensive understanding of climate conditions during the 19th and 20th centuries.

67

68 **2 Data and Methods**

69 2.1 Climate of the Study Area

70

71 The study area, which spans 36–42° N and 26–38° E, was based on the distribution of available
72 tree-ring chronologies. This vast area covers much of western Anatolia and includes the western
73 Black Sea, Marmara, and western Mediterranean regions. Much of this area is characterized by a
74 Mediterranean climate that is primarily controlled by polar and tropical air masses (Türkeş 1996,
75 Deniz et al. 2011). In winter, polar fronts from the Balkan Peninsula bring cold air that is
76 centered in the Mediterranean. Conversely, the dry, warm conditions in summer are dominated
77 by weak frontal systems and maritime effects. Moreover, the Azores high-pressure system in
78 summer and anticyclonic activity from the Siberian high-pressure system often cause below
79 normal precipitation and dry sub-humid conditions over the region (Türkeş 1999, Deniz et al.
80 2011). In this Mediterranean climate, annual mean temperature and precipitation range from 3.6
81 °C to 20.1 °C and from 295 to 2220 mm, respectively, both of which are strongly controlled by
82 elevation (Deniz et al. 2011).

83

84

85

86



87 2.2 Development of tree-ring chronologies

88

89 To investigate past temperature conditions, we used a network of 23 tree-ring site chronologies
90 (Fig. 1). Fifteen chronologies were produced by previous investigations that focused on
91 reconstructing precipitation in the study area. In addition, we sampled eight new study sites and
92 developed tree-ring time series for these areas (Table 1). Increment cores were taken from living
93 *Pinus nigra* Arn. and *Pinus sylvestris* L. trees and cross-sections were taken from *Abies*
94 *nordmanniana* (Steven) Spach and *Picea orientalis* (L.) Link trees.

95

96 Samples were processed using standard dendrochronological techniques (Stokes & Smiley 1968,
97 Orvis & Grissino-Mayer 2002, Speer 2010). Tree-ring widths were measured, then visually
98 crossdated using the list method (Yamaguchi 1991). We used the computer program COFECHA,
99 which uses segmented time-series correlation techniques, to statistically confirm our visual
100 crossdating (Holmes 1983, Grissino-Mayer 2001). Crossdated tree-ring time series were then
101 standardized by fitting a 67% cubic smoothing spline with a 50% cutoff frequency to remove
102 non-climatic trends related to the age, size, and the effects of stand dynamics using the ARSTAN
103 program (Cook 1985, Cook et al. 1990a). These detrended series were then pre-whitened with
104 low-order autoregressive models to remove persistence not related to climatic variations. For
105 each chronology, the individual measured series were averaged to a single chronology by
106 computing the biweight robust means to reduce the influences of outliers (Cook et al. 1990b).
107 The mean sensitivity, which is a metric representing the year-to-year variation in ring width
108 (Fritts 1976), was calculated for each chronology and compared. The minimum sample depth for
109 each chronology was determined according to expressed population signal (EPS), which we used



110 as a guide for assessing the likely loss of reconstruction accuracy. Although arbitrary, we
111 required the commonly considered threshold of $EPS > 0.85$ (Wigley et al. 1984; Briffa & Jones
112 1990).

113

114 2.3 Temperature reconstruction

115

116 We extracted monthly temperature and precipitation records from the climate dataset CRU TS
117 3.23 gridded at 0.5° intervals (Jones and Harris 2008) from KNMI Climate Explorer
118 (<http://climexp.knmi.nl>) for $36\text{--}42^\circ\text{N}$, $26\text{--}38^\circ\text{E}$. The period AD 1930–2002 was chosen for the
119 analysis because it maximized the number of station records within the study area.

120

121 First, the climate-growth relationships were investigated with response function analysis (RFA)
122 (Fritts 1976) for biological year from previous October to current October using the
123 DENDROCLIM2002 program (Biondi & Waikul 2004). This analysis is done to determine the
124 months during which the tree-growth is the most responsive to temperature. Second, the climate
125 reconstruction is performed by regression based on the principal component (PCs) of the 23
126 chronologies within the study area. The significant PCs were selected by stepwise regression.

127 The regression equation is calibrated on the common period (1930–2002) between robust
128 temperature time-series and the selected tree-ring series. Third, the final reconstruction is based
129 on bootstrap regression (Till and Guiot, 1990), the best method to assess the quality of the
130 regression and to calculate appropriate confidence intervals. It consists in randomly resampling
131 the calibration datasets to produce 1000 calibration equations based on a number of slightly
132 different datasets.



133 The quality of the reconstruction is assessed by a number of standard statistics. The overall
134 quality of fit of reconstruction is evaluated based on the determination coefficient (R^2), which
135 expresses the percentage of variance explained by the model and the root mean squared error
136 (RMSE), which expresses the calibration error. This does not insure the quality of the
137 extrapolation which needs additional statistics based on independent observations, i.e.
138 observations not used by the calibration (verification data). They are provided by the
139 observations not resampled by the bootstrap process. The prediction RMSE (called RMSEP), the
140 reduction of error (RE) and the coefficient of efficiency (CE) are calculated on the verification
141 data and enable to test the predictive quality of the calibrated equations (Cook et al, 1994).
142 Traditionally, a positive RE or CE values means a statistically significant reconstruction model,
143 but bootstrap is much more interesting as it produces confidence intervals and finally we accept
144 the RE and CE which are significantly larger than zero, which is more constraining than being
145 just positive in mean. An early common period (1902–1929) is available for additional
146 verification, during which some climatic series are available but are not of sufficient quality to
147 insure an optimal calibration.

148

149 To identify the extreme March–April cold and warm events in the reconstruction, standard
150 deviation (SD) values were used. Years one and two SD above and below the mean were
151 identified as warm, very warm, cold, and very cold years, respectively. Finally, as a way to
152 assess the spatial representation of our temperature reconstruction, we conducted a spatial field
153 correlation analysis between reconstructed values and the gridded CRU TS3.23 temperature field
154 (Jones and Harris 2008) for a broad region of the Mediterranean over the early common period
155 (1901–1929), and over the entire instrumental period (ca. 1901–2002).



156

157 **3 Results and Discussion**

158 3.1 Tree-ring chronologies

159 In addition to 15 chronologies developed by previous studies, we produced six *P. nigra*, one *P.*
160 *sylvestris*, one *A. nordmanniana* / *P. orientalis* chronologies for this study (Table 2). The Çorum
161 district produced two *P. nigra* chronologies: one the longest (KAR; 627 years long) and the other
162 the most sensitive to climate (SAH; mean sensitivity value of 0.25). Previous investigations of
163 climate-tree growth relationships reported a mean sensitivity range of 0.13–0.25 for *P. nigra* in
164 Turkey (Köse 2011, Akkemik et al. 2008). The KAR, SAH, and ERC chronologies (with mean
165 sensitivity values from 0.22 to 0.25) were classified as very sensitive, and the SAV, HCR, and
166 PAY chronologies (mean sensitivity values range 0.17–0.18) contained values characteristic of
167 being sensitive to climate. The lowest mean sensitivity value was obtained for the ART *A.*
168 *nordmanniana* / *P. orientalis* chronology. Nonetheless, this chronology retained a statistically
169 significant temperature signal ($p < 0.05$).

170

171 3.2 March-April temperature reconstruction

172 RFA coefficients of May to August precipitation are positively correlated with most of the tree-
173 ring series (Fig. 2) and among them, May and June coefficients are generally significant. The
174 first principal component of the 23 chronologies, which explains 47% of the tree-growth
175 variance, is highly correlated with May–August total precipitation, statistically ($r = 0.65$, $p \leq$
176 0.001) and visually (Fig. 3). The high correlation was expected given that numerous studies also
177 found similar results in Turkey (Akkemik 2000a, Akkemik 2000b, Akkemik 2003, Akkemik et



178 al. 2005, Akkemik & Aras 2005, Hughes et al. 2001, D'Arrigo & Cullen 2001, Touchan et al.
179 2003; Touchan et al. 2005a, Touchan et al. 2005b, Touchan et al. 2007, Köse et al. 2011).

180

181 The influence of temperature was not as strong as May–August precipitation on radial growth,
182 although generally positive in early spring (March and April) (Fig. 2). Conversely, the ART
183 chronology from northeastern Turkey contained a strong temperature signal, which was
184 significantly positive in March. In addition to this chronology, we also used the chronologies that
185 revealed the influence of precipitation, as well as temperature to reconstruct March–April
186 temperature.

187

188 The higher order PCs of the 23 chronologies are significantly correlated with the March–April
189 temperature and, by nature, are independent on the precipitation signal (Table 3). The best
190 selection for fit temperature are obtained with the PC₃, PC₄, PC₅, PC₇, PC₉, PC₁₀, PC₁₅, PC₁₇,
191 PC₂₁, which explains together 25% of the tree-ring chronologies. So the temperature signal
192 remains important in the tree-ring chronologies and can be reconstructed. The advantage to
193 separate both signals through orthogonal PCs enable to remove an unwanted noise for our
194 temperature reconstruction. Thus, PC₁ was not used as potential predictor of temperature because
195 it is largely dominated by precipitation (Table 3, Fig. 3). The last two PCs contain a too small
196 part of the total variance to be used in the regressions. However, even if Jolliffe (1982) and Hadi
197 & Ling (1998) claimed that certain PCs with small eigenvalues (even the last one), which are
198 commonly ignored by principal components regression methodology, may be related to the
199 independent variable, we must be cautious with that because they may be much more dominated
200 by noise than the first ones. So, the contribution of each PC to the regression sum of squares is



201 also important for selection of PCs (Hadi & Ling 1998). The findings of Jolliffe (1982) and Hadi
202 & Ling (1998) provide a justification for using non-primary PCs, (*e.g.*, of second and higher
203 order) in our regression, given that correlations with temperature may be over-powered by
204 affects from precipitation in our study area (Cook 2011, personal communication).

205

206 Using this method, the calibration and verification statistics indicated a statistically significant
207 reconstruction (Table 4, Fig. 4). The regression model for the calibration period was:

208

209 Eq. (1): $TMP = 7.53 - 2.94PC_3 + 4.02PC_4 + 2.50PC_5 + 2.77PC_7 + 2.73PC_9 - 2.67PC_{10} -$

210 $5.17PC_{15} + 1.98PC_{17} - 5.82PC_{21}$

211

212 The regression model accounted for 67% (Adj. $R^2 = 0.64$, $p \leq 0.0001$) of the actual temperature
213 variance over the calibration period (1930–2002). Also, actual and reconstructed March–April
214 temperature values had nearly identical trends during the period 1930–2002 (Fig. 4). Moreover, the tree-
215 ring chronologies successfully simulated both high frequency and warming trends in the temperature data
216 during this period. The reconstruction was more powerful at classifying warm events rather than cold
217 events. Over the last 73 years, eight of ten warm events in the instrumental data were also observed in
218 the reconstruction, while five of nine cold events were captured. Similarly, previous tree-ring based
219 precipitation reconstructions for Turkey (Köse et al. 2011; Akkemik et al. 2008) were generally
220 more successful in capturing dry years rather than wet years.

221

222 Our temperature reconstruction on the 1800–2002 period is obtained by bootstrap regression,
223 using 1000 iterations (Fig. 5). The confidence intervals are obtained from the range between the



224 2.5th and the 97.5th percentiles of the 1000 simulations. For the pre-instrumental period (1800–
225 1929), a total of 23 cold (1813, 1818, 1821, 1824, 1837, 1848, 1854, 1858, 1860, 1869, 1877–
226 1878, 1880–1881, 1883, 1897–1898, 1905–1907, 1911–1912, 1923) and 13 warm (1801–1802,
227 1807, 1845, 1853, 1866, 1872–1873, 1879, 1885, 1890, 1901, 1926) events were determined.
228 After comparing our results with event years obtained from May–June precipitation
229 reconstructions from western Anatolia (Köse et al. 2011), the cold years 1818, 1848, and 1897
230 appeared to coincide with wet years and 1881 was a very wet year for the entire region.
231 Furthermore, these years can be described as cold (in March–April) and wet (in May–June) for
232 western Anatolia.
233
234 Spatial correlation analysis revealed that our network-based temperature reconstruction was
235 representative of conditions across Turkey, as well as the broader Mediterranean region (Fig. 6).
236 During the period 1901–2002, estimated temperature values were highly significant (r range 0.5–
237 0.6, $p < 0.01$) with instrumental conditions recorded from southern Ukraine to the west across
238 Romania, and from northern areas of Libya and Egypt to the east across Iraq. The strength of the
239 reconstruction model is evident in the broad spatial implications demonstrated by the
240 temperature record. Thus, we interpret warm and cold periods and extreme events within the
241 record with high confidence.
242
243 Among the warm periods in our reconstruction, conditions during the year 1879 were dry, 1895
244 wet, and 1901 very wet across the broad region of western Anatolia (Köse et al. 2011). Hence,
245 we defined 1879 as a warm (in March–April) and dry year (in May–June), and 1895 and 1901
246 were warm and wet years. In the years 1895 and 1901 the combination of a warm early spring



247 and a wet late spring-summer caused enhanced radial growth in Turkey, interpreted as longer
248 growing seasons without drought stress.

249

250 Of these event years, 1897 and 1898 were exceptionally cold and 1845, 1872 and 1873 were
251 exceptionally warm. During the last 200 years, our reconstruction suggests that the coldest year
252 was 1898 and the warmest year was 1873. The reconstructed extreme events also coincided with
253 accounts from historical records. Server (2008) recounted the winter of 1898 as characterized by
254 anomalously cold temperatures that persisted late into the spring season. A family, who brought
255 their livestock herds up into the plateau region in Kırşehir seeking food and water were suddenly
256 covered in snow on 11 March 1898. This account of a late spring freeze supports the
257 reconstruction record of spring temperatures across Turkey, and offers corroboration to the
258 quality of the reconstructed values.

259

260 Seyf (1985) reported that extreme summer temperature during the year 1873 resulted in
261 widespread crop failure and famine. Historical documents recorded an infamous drought-derived
262 famine that occurred in Anatolia from 1873 to 1874 (Quataert, 1996, Kuniholm, 1990), which
263 claimed the lives of 250,000 people and a large number of cattle and sheep (Faroqhi, 2009). This
264 drought caused widespread mortality of livestock and depopulation of rural areas through human
265 mortality, and migration of people from rural to urban areas. Further, the German traveler
266 Naumann (1893) reported a very dry and hot summer in Turkey during the year 1873 (Heinrich
267 et al, 2013). Conditions worsened when the international stock exchanges crashed in 1873,
268 marking the beginning of the "Great Depression" in the European economy (Zürcher, 2004). Our
269 temperature record suggests that dry conditions during the early 1870s were possibly exacerbated



270 by warm spring temperatures that likely carried into summer. A similar pattern of intensified
271 drought by warm temperatures was demonstrated recently by Griffin and Anchukaitis (2014) for
272 the current drought in California, USA.

273

274 Extreme cold and warm events were usually one year long, and the longest extreme cold and
275 warm events were two and three years, respectively. These results were similar with durations of
276 extreme wet and dry events in Turkey (Touchan et al. 2003, Touchan et al. 2005a, Touchan et al.
277 2005b, Touchan et al. 2007, Akkemik & Aras, 2005, Akkemik et al. 2005, Akkemik et al. 2008,
278 Köse et al. 2011). Moreover, seemingly innocuous short-term warm events, such as the 1807
279 event, were recorded across the Mediterranean and in high elevations of the European regions.
280 Casty et al. (2005) reported the year 1807 as being one of the warmest alpine summers in the
281 European Alps over the last 500 years. As such, a drought record from Nicault et al. (2008)
282 echoes this finding, as a broad region of the Mediterranean basin experienced drought
283 conditions.

284

285 Low frequency variability of our spring temperature reconstruction showed larger variability in
286 nineteenth century than twentieth century. Similar results observed on previous tree-ring based
287 precipitation reconstructions from Turkey (Touchan et al. 2003, D'Arrigo et al. 2001, Akkemik
288 and Aras 2005, Akkemik et al. 2005, Köse et al. 2011). Moreover, cold periods observed in our
289 reconstruction are generally appeared as generally wet in the precipitation reconstructions, while
290 warm periods generally correlated with dry periods (Fig. 7).

291



292 Heinrich et al. (2013) analyzed winter-to-spring (January–May) air temperature variability in
293 Turkey since AD 1125 as revealed from a robust tree-ring carbon isotope record from *Juniperus*
294 *excelsa*. Although they offered a long-term perspective of temperature over Turkey, the
295 reconstruction model, which covered the period 1949–2006, explained 27% of the variance in
296 temperature since the year 1949. In this study, we provided a short-term perspective of
297 temperature fluctuation based on a robust model (calibrated and verified 1930–2002; Adj. $R^2 =$
298 0.64; $p \leq 0.0001$). Yet, the Heinrich et al. (2013) temperature record did not capture the 20th
299 century warming trend as found elsewhere (Wahl et al. 2010). However, their temperature trend
300 does agree with trend analyses conducted on meteorological data from Turkey and other areas in
301 the eastern Mediterranean region. The warming trend seen during our reconstruction calibration
302 period (1930–2002) was similar to the data shown by Wahl et al. (2010) across the region and
303 hemisphere. Further, the warming trends seen in our record agrees with data presented by Turkes
304 & Sumer (2004), of which they attributed to increased urbanization in Turkey. Considering long-
305 term changes in spring temperatures, the 19th century was characterized by more high-frequency
306 fluctuations compared to the 20th century, which was defined by more gradual changes and
307 includes the beginning of decreased DTRs in the region (Turkes & Sumer, 2004).

308

309 **4 Conclusions**

310

311 In this study, we used a broad network of tree-ring chronologies to provide the first tree-ring
312 based temperature reconstruction for Turkey and identified extreme cold and warm events during
313 the period 1800–1929 CE. Similar to the precipitation reconstructions against which we compare
314 our air temperature record, extreme cold and warm years were generally short in duration (one



315 year) and rarely exceeded two-three years in duration. The coldest and warmest years over
316 western Anatolia were experienced during the 19th century, and the 20th century is marked by a
317 temperature increase.

318

319 Reconstructed temperatures for the 19th century suggest that more short-term fluctuations
320 occurred compared to the 20th century. The gradual warming trend shown by our reconstruction
321 calibration period (1930–2002) is coeval with decreases in spring DTRs. Given the results of
322 Turkes and Sumer (2004), the variations in short- and long-term temperature changes between
323 the 19th and 20th centuries might be related to increased urbanization in Turkey.

324

325 The study revealed the potential for reconstructing temperature in an area previously thought
326 impossible, especially given the strong precipitation signals displayed by most tree species
327 growing in the dry Mediterranean climate that characterizes broad areas of Turkey. Our
328 reconstruction only spans 205 years due to the shortness of the common interval for the
329 chronologies used in this study, but the possibility exists to extend our temperature
330 reconstruction further back in time by increasing the sample depth with more temperature-
331 sensitive trees, especially from northeastern Turkey. Thus future research will focus on
332 increasing the number of tree-ring sites across Turkey, and maximizing chronology length at
333 existing sites that would ultimately extend the reconstruction back in time.

334

335

336

337



338 **Acknowledgements**

339

340 This research was supported by The Scientific and Technical Research Council of Turkey
341 (TUBITAK); Projects ÇAYDAG 107Y267 and YDABAG 102Y063. N. Köse was supported by
342 The Council of Higher Education of Turkey. We are grateful to the Turkish Forest Service
343 personnel and Ali Kaya, Umut Ç. Kahraman and Hüseyin Yurtseven for their invaluable support
344 during our field studies. J. Guiot was supported by the Labex OT-Med (ANR-11-LABEX-0061),
345 French National Research Agency (ANR).

346



347 **References**

- 348 Akkemik, Ü.: Dendroclimatology of Umbrella pine (*Pinus pinea* L.) in Istanbul (Turkey), Tree-
349 Ring Bull., 56, 17–20, 2000a.
- 350 Akkemik, Ü.: Tree-ring chronology of *Abies cilicica* Carr. in the Western Mediterranean Region
351 of Turkey and its response to climate, Dendrochronologia, 18, 73–81, 2000b.
- 352 Akkemik, Ü.: Tree-rings of *Cedrus libani* A. Rich the northern boundary of its natural
353 distribution, IAWA J, 24(1), 63-73, 2003.
- 354 Akkemik, Ü. and Aras, A.: Reconstruction (1689–1994) of April–August precipitation in
355 southwestern part of central Turkey, Int. J. Clim., 25, 537–548, 2005.
- 356 Akkemik, Ü., Dagdeviren, N., and Aras, A.: A preliminary reconstruction (A.D. 1635–2000) of
357 spring precipitation using oak tree rings in the western Black Sea region of Turkey, Int. J.
358 Biomet., 49(5), 297–302, 2005.
- 359 Akkemik, Ü., D’Arrigo, R., Cherubini, P., Köse, N., and Jacoby, G.: Tree-ring reconstructions of
360 precipitation and streamflow for north-western Turkey, Int. J. Clim., 28, 173–183, 2008.
- 361 Biondi, F. and Waikul, K.: DENDROCLIM2002: A C++ program for statistical calibration of
362 climate signals in tree-ring chronologies, Comp. Geosci., 30, 303–311, 2004.
- 363 Briffa, K. R. and Jones, P. D.: Basic chronology statistics and assessment. In: Methods of
364 Dendrochronology: Applications in the Environmental Sciences (Cook, E. and Kairiukstis, L.
365 A. eds). Kluwer Academic Publishers, Amsterdam, pp. 137–152, 1990.
- 366 Casty, C., Wanner, H., Luterbacher, J., Esper, J., and Böhm, R.: Temperature and precipitation
367 variability in the European Alps since 1500, Int. J. Clim., 25(14), 1855–1880, 2005.



- 368 Cook, E.: A time series analysis approach to tree-ring standardization. PhD. Dissertation.
369 University of Arizona, Tucson, 1985.
- 370 Cook, E., Briffa, K., Shiyatov, S., and Mazepa, V.: Tree-ring standardization and growth-trend
371 estimation. In: *Methods of Dendrochronology: Applications in the Environmental Sciences*
372 (Cook, E. and Kairiukstis, L. A. eds). Kluwer Academic Publishers, Amsterdam, pp.104–
373 122, 1990a.
- 374 Cook, E., Shiyatov, S., and Mazepa, V.: Estimation of the mean chronology. In: *Methods of*
375 *Dendrochronology: Applications in the Environmental Sciences* (Cook, E. and Kairiukstis, L.
376 A. eds). Kluwer Academic Publishers, Amsterdam, pp. 123–132, 1990b.
- 377 D'Arrigo, R. and Cullen, H. M.: A 350-year (AD 1628–1980) reconstruction of Turkish
378 precipitation. *Dendrochronologia*, 19(2), 169–177, 2001.
- 379 Deniz, A., Toros, T., and Incecik, S.: Spatial variations of climate indices in Turkey, *Int. J.*
380 *Clim.*, 31, 394-403, 2011.
- 381 Fritts, H. C.: *Tree Rings and Climate*. Academic Press, New York, 1976.
- 382 Griggs, C., DeGaetano, A., Kuniholm, P., and Newton, M.: A regional high-frequency
383 reconstruction of May–June precipitation in the north Aegean from oak tree rings, A.D.
384 1809–1989, *Int. J. Clim.*, 27, 1075–1089, 2007.
- 385 Grissino-Mayer, H. D.: Evaluating crossdating accuracy: A manual and tutorial for the computer
386 program COFECHA, *Tree-Ring Res.*, 57, 205–221, 2001.
- 387 Griffin, D. and Anchukaitis, K. J.: How unusual is the 2012–2014 California drought? *Geophys.*
388 *Res. Lett.*, 41(24), 9017–9023, 2014.



- 389 Hadi, A. S. and Ling, R. F.: Some cautionary notes on the use of principal components
390 regression, *Amer. Statist.*, 52(1), 15–19, 1998.
- 391 Heinrich, I., Touchan, R., Liñán, I. D., Vos, H., and Helle, G.: Winter-to-spring temperature
392 dynamics in Turkey derived from tree rings since AD 1125, *Clim. Dynam.*, 41(7–8), 1685–
393 1701, 2013.
- 394 Holmes, R. L.: Computer-assisted quality control in tree-ring data and measurements, *Tree-Ring*
395 *Bull.*, 43, 69–78, 1983.
- 396 Hughes, M. K., Kuniholm, P. I., Garfin, G. M., Latini, C., and Eischeid, J.: Aegean tree-ring
397 signature years explained, *Tree-Ring Res.*, 57(1), 67–73, 2001.
- 398 Jolliffe, I. T.: A note on the use of principal components in regression, *Appl. Stat.*, 31(3), 300–
399 303, 1982.
- 400 Jones, P. D. and Harris, I.: Climatic Research Unit (CRU) time-series datasets of variations in
401 climate with variations in other phenomena. NCAS British Atmospheric Data Centre, 2008.
402 <http://catalogue.ceda.ac.uk/uuid/3f8944800cc48e1cbc29a5ee12d8542d>
- 403 Köse, N., Akkemik, Ü., and Dalfes, H. N.: Anadolu'nun iklim tarihinin son 500 yılı:
404 Dendroklimatolojik ilk sonuçlar. Türkiye Kuvaterner Sempozyumu-TURQUA-V, 02–03
405 Haziran 2005, *Bildiriler Kitabı*, 136–142 (In Turkish), 2005.
- 406 Köse, N., Akkemik, Ü., Dalfes, H. N., and Özeren, M. S.: Tree-ring reconstructions of May–June
407 precipitation of western Anatolia, *Quat. Res.*, 75, 438–450, 2011.
- 408 Meko, D. M. and Graybill, D. A.: Tree-ring reconstruction of upper Gila River discharge, *Wat.*
409 *Res. Bull.*, 31, 605–616, 1995.



- 410 Mutlu, H., Köse, N., Akkemik, Ü., Aral, D., Kaya, A., Manning, S. W., Pearson, C. L., and
411 Dalfes, N.: Environmental and climatic signals from stable isotopes in Anatolian tree rings,
412 Turkey, Reg. Environ. Change, doi: 10.1007/s1011301102732, 2011.
- 413 Nicault, A., Alleaume, S., Brewer, S., Carrer, M., Nola, P., and Guiot, J.: Mediterranean drought
414 fluctuation during the last 500 years based on tree-ring data, Clim. Dynam., 31(2–3), 227–
415 245, 2008.
- 416 Orvis, K. H. and Grissino-Mayer, H. D.: Standardizing the reporting of abrasive papers used to
417 surface tree-ring samples, Tree-Ring Res., 58, 47–50, 2002.
- 418 Server, M.: Evaluation of an oral history text in the context of social memory and traditional
419 activity, Milli Folklor 77, 61–68 (In Turkish), 2008.
- 420 Speer, J. H.: Fundamentals of Tree-Ring Research, University of Arizona Press, Tucson, 2010.
- 421 Stokes, M. A. and Smiley, T. L.: An Introduction to Tree-ring Dating, The University of Arizona
422 Press, Tucson, 1996.
- 423 Till, C. and Guiot, J.: Reconstruction of precipitation in Morocco since A D 1100 based on
424 *Cedrus atlantica* tree-ring widths, Quat. Res., 33, 337–351, 1990.
- 425 Touchan, R., Garfin, G. M., Meko, D. M., Funkhouser, G., Erkan, N., Hughes, M. K., and
426 Wallin, B. S.: Preliminary reconstructions of spring precipitation in southwestern Turkey
427 from tree-ring width, Int. J. Clim., 23, 157–171, 2003.
- 428 Touchan, R., Xoplaki, E., Funkhouser, G., Luterbacher, J., Hughes, M. K., Erkan, N., Akkemik,
429 Ü., and Stephan, J.: Reconstruction of spring/summer precipitation for the Eastern
430 Mediterranean from tree-ring widths and its connection to large-scale atmospheric
431 circulation, Clim. Dynam., 25, 75–98, 2005a.



- 432 Touchan, R., Funkhouser, G., Hughes, M. K., and Erkan, N.: Standardized Precipitation Index
433 reconstructed from Turkish ring widths, *Clim. Change*, 72, 339–353, 2005b.
- 434 Touchan, R., Akkemik, Ü., Huges, M. K., and Erkan, N.: May–June precipitation reconstruction
435 of southwestern Anatolia, Turkey during the last 900 years from tree-rings, *Quat. Res.*, 68,
436 196–202, 2007.
- 437 Turkes, M.: Spatial and temporal analysis of annual rainfall variations in Turkey. *Int. J. Clim.*,
438 16, 1057–1076, 1996.
- 439 Turkes, M.: Vulnerability of Turkey to desertification with respect to precipitation and aridity
440 conditions. *Turk. J. Engineer. Environ Sci.*, 23, 363–380, 1999.
- 441 Turkes, M. and Sumer, U. M.: Spatial and temporal patterns of trends variability in diurnal
442 temperature ranges of Turkey. *Theor. Appl. Clim.*, 77, 195–227, 2004.
- 443 Wahl, E. R., Anderson, D. M., Bauer, B. A., Buckner, R., Gille, E. P., Gross, W. S., Hartman,
444 M., and Shah, A.: An archive of high-resolution temperature reconstructions over the past
445 two millennia, *Geochem. Geophys. Geosyst.*, 11, Q01001, doi:10.1029/2009GC002817,
446 2010.
- 447 Wigley, T. M. L., Briffa, K. R., and Jones, P. D.: On the average value of correlated time series
448 with applications in dendroclimatology and hydrometeorology, *J. Clim. Appl. Met.*, 23, 201–
449 213, 1984.
- 450 Yamaguchi, D. K.: A simple method for cross-dating increment cores from living trees. *Can. J.*
451 *For. Res.*, 21, 414–416, 1991.



452 Table 1. Site information for the new chronologies developed by this study in Turkey.

Site name	Site code	Species	No. trees/ cores	Aspect	Elev. (m)	Lat. (N)	Long. (E)
Çorum, Kargı, Karakise kayalıkları	KAR	<i>Pinus nigra</i>	22 / 38	SW	1522	41°11'	34°28'
Çorum, Kargı, Şahinkayası mevki	SAH	<i>P. nigra</i>	12 / 21	S	1300	41°13'	34°47'
Bilecik, Muratdere	ERC	<i>P. nigra</i>	12 / 25	SE	1240	39°53'	29°50'
Bolu, Yedigöller, Ayıkaya mevki	BOL	<i>P. sylvestris</i>	10 / 20	SW	1702	40°53'	31°40'
Eskişehir, Mihaliççık, Savaş alanı mevki	SAV	<i>P. nigra</i>	10 / 18	S	1558	39°57'	31°12'
Kayseri, Aladağlar milli parkı, Hacer ormanı	HCR	<i>P. nigra</i>	18 / 33	S	1884	37°49'	35°17'
Kahramanmaraş, Göksun, Payanburnu mevki	PAY	<i>P. nigra</i>	10 / 17	S	1367	37°52'	36°21'
Artvin, Borçka, Balcı işletmesi	ART	<i>Abies nordmanniana</i> <i>Picea orientalis</i>	23 / 45	N	1200– 2100	41°18'	41°54'

453

454



455 Table 2. Summary statistics for the new chronologies developed by this study in Turkey.

Site Code	Total chronology			Common interval		
	Time span	1st year (*EPS > 0.85)	Mean sensitivity	Time span	Mean correlations: among radii /between radii and mean	Variance explained by PC1 (%)
KAR	1307– 2003	1620	0.22	1740–1994	0.38 / 0.63	41
SAH	1663– 2003	1738	0.25	1799–2000	0.42 / 0.67	45
ERC	1721– 2008	1721	0.23	1837–2008	0.45 / 0.69	48
BOL	1752– 2009	1801	0.18	1839–1994	0.32 / 0.60	36
SAV	1630– 2005	1700	0.17	1775–2000	0.33 / 0.60	38
HCR	1532– 2010	1704	0.18	1730–2010	0.38 / 0.63	40
PAY	1537– 2010	1790	0.18	1880–2010	0.28 / 0.56	32
ART	1498– 2007	1624	0.12	1739–1996	0.37 / 0.60	41

456 *EPS = Expressed Population Signal [Wigley et al., 1984]

457



458 Table 3. Statistics from reconstruction model principal components analysis.

	Explained variance (%)	Correlation coefficients with	
		May–August PPT	March–April TMP
PC1	46.57	−0.65	−0.19
PC2	7.86	−0.07	0.15
PC3*	4.93	0.04	−0.48
PC4*	4.68	0.11	0.17
PC5*	4.42	−0.25	0.27
PC6	3.73	0.15	−0.14
PC7*	3.56	0.19	0.18
PC8	2.87	0.26	0.01
PC9*	2.45	0.16	0.17
PC10*	2.21	0.14	−0.08
PC11	2.09	−0.36	−0.20
PC12	1.80	−0.12	0.05
PC13	1.63	−0.06	0.17
PC14	1.55	−0.14	0.06
PC15*	1.50	−0.20	−0.14
PC16	1.31	0.04	0.08
PC17*	1.25	0.15	0.19
PC18	1.14	0.13	0.02
PC19	1.09	0.16	−0.11
PC20	0.95	−0.15	−0.01
PC21*	0.89	0.06	−0.28
PC22	0.85	0.44	0.10
PC23	0.67	−0.22	−0.02

459 “*” indicates the PCs, which used in the
 460 reconstruction as predictors

461

462

463

464

465

466

467



468 Table 4. Calibration and verification statistics of bootstrap method (1000 iterations
469 applied) showing the mean values based on the 95% confidence interval (CI)

			470
Mean (95% CI)			
Calibration	RMSE	0.65 (0.52; 0.77)	471
	R^2	0.73 (0.60; 0.83)	472
Verification	RE	0.54 (0.15; 0.74)	473
	CE	0.51 (0.04; 0.72)	474
	RMSEP	0.88 (0.67; 1.09)	475
			476

477 *RMSE* root mean squared error; R^2 coefficient of determination; *RE* reduction of error; *CE*
478 coefficient of efficiency; *RMSEP* root mean squared error prediction

479

480

481

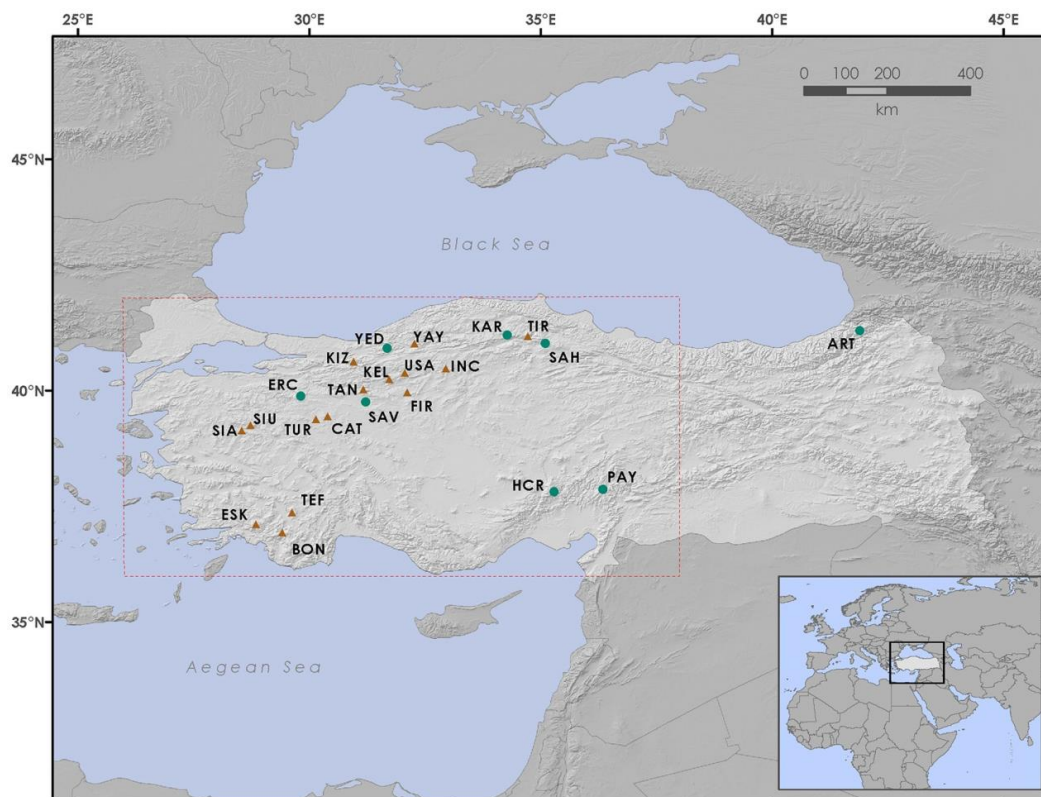
482

483

484

485

486

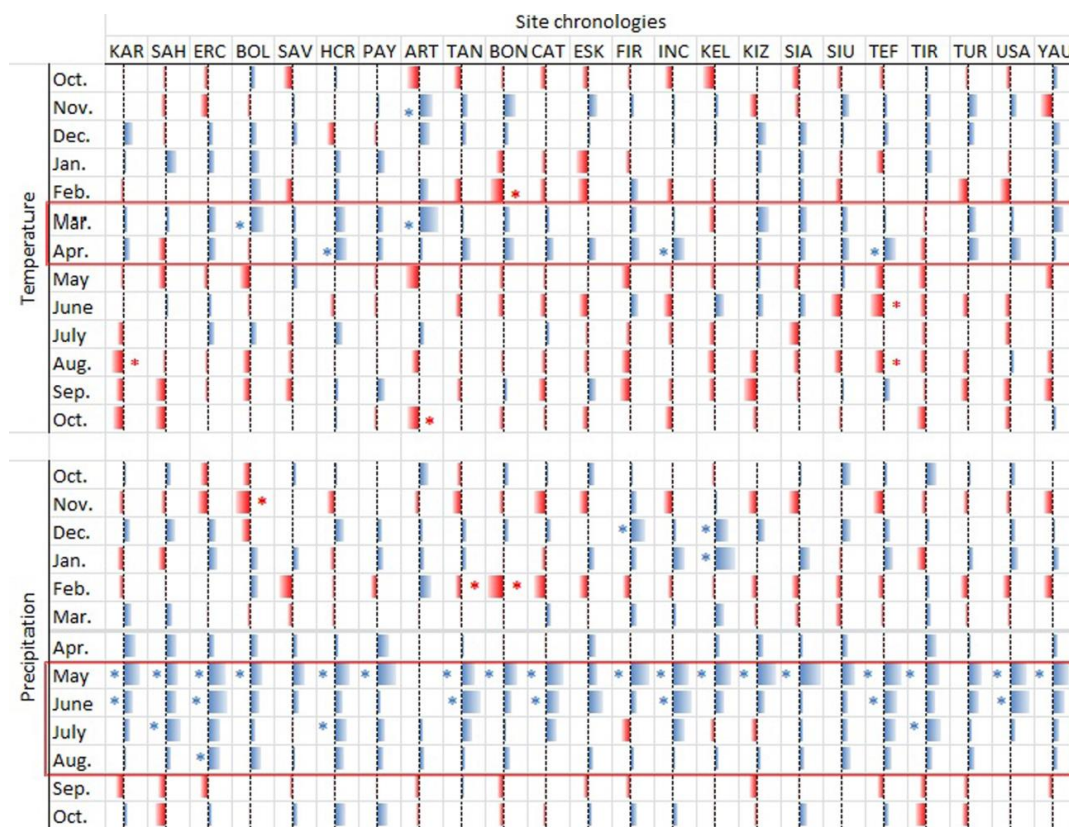


487
488 **Figure 1.** Tree-ring chronology sites in Turkey used to reconstruct temperature. Circles
489 represent the new sampling efforts from this study and the triangles represent previously-
490 published chronologies (YAY, SIA, SIU: Mutlu et al. 2011; TIR: Akkemik et al. 2008; TAN:
491 Köse et al. unpublished data; KIZ, ESK, TEF, BON, KEL, USA, FIR, TUR: Köse et al. 2011;
492 CAT, INC: Köse et al. 2005). The box (dashed line) represents the area for which the
493 temperature reconstruction was performed.

494

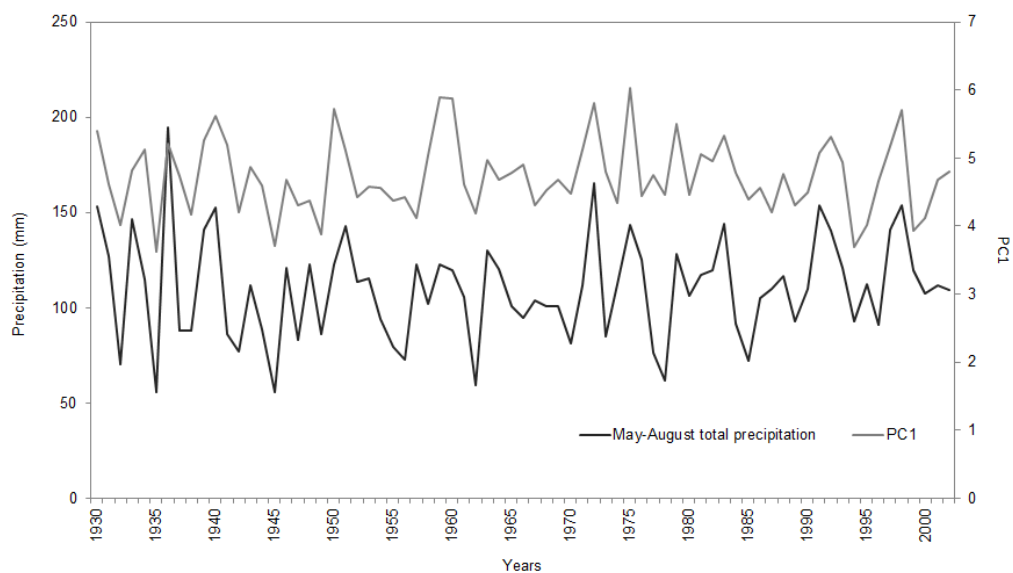
495

496



497

498 **Figure 2.** Summary of response function results of 23 chronologies. Red color represents
 499 negative effects of climate variability on tree ring width; blue color represents positive effects of
 500 climate variability on tree ring width. “*” indicates statistically significant response function
 501 confidents ($p \leq 0.05$). Each response function includes 13 weights for average monthly
 502 temperatures and 13 monthly precipitations from October of the prior year to October of current
 503 year.



504

505 **Figure 3.** The comparison of May-August total precipitation (mm) and the first principal

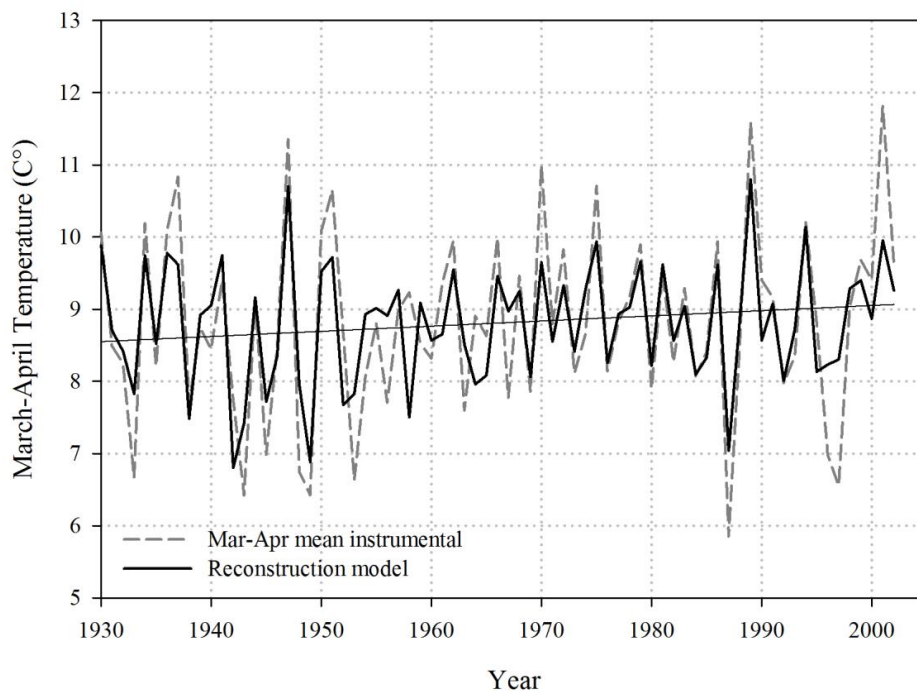
506 component of 23 tree-ring chronologies.

507

508

509

510



511

512 **Figure 4.** Actual (instrumental) and reconstructed March–April temperature (°C). Dashed lines
513 (dark grey) represent actual values and solid lines (black) represent reconstructed values shown
514 with trend line (linear black line). Note: y-axes labels range 5–13 °C.

515

516

517

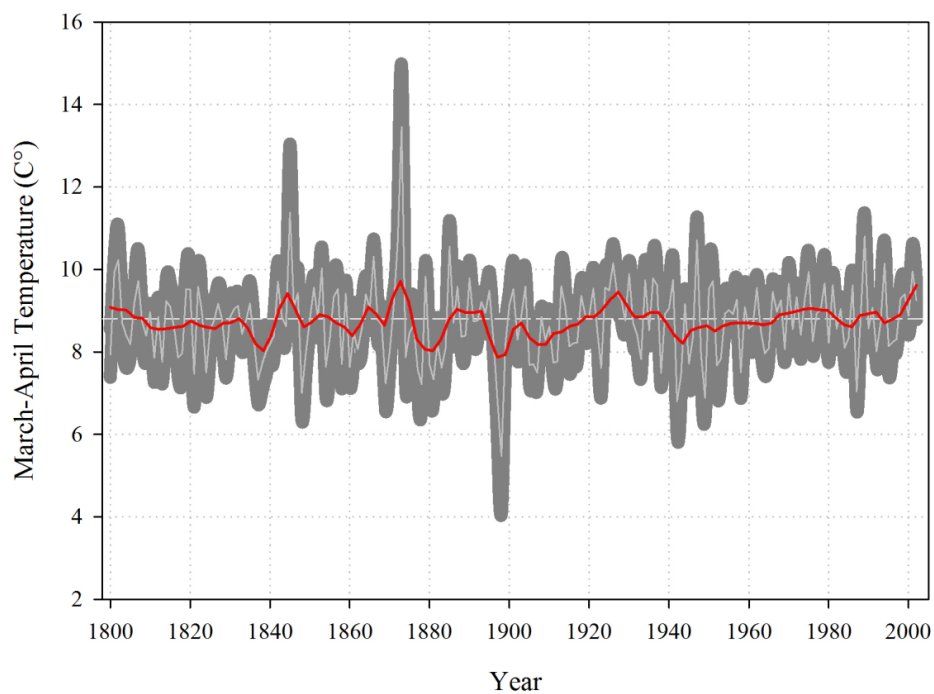
518

519

520

521

522



523

524 **Figure 5.** March–April temperature reconstruction for Turkey for the period 1800–2002

525 CE. The central horizontal line (dashed white) shows the reconstructed long-term mean;

526 dark grey background denotes Monte Carlo ($n = 1000$) bootstrapped 95% confidence

527 limits; and the solid black line shows 13-year low-pass filter values. Note: y-axis labels

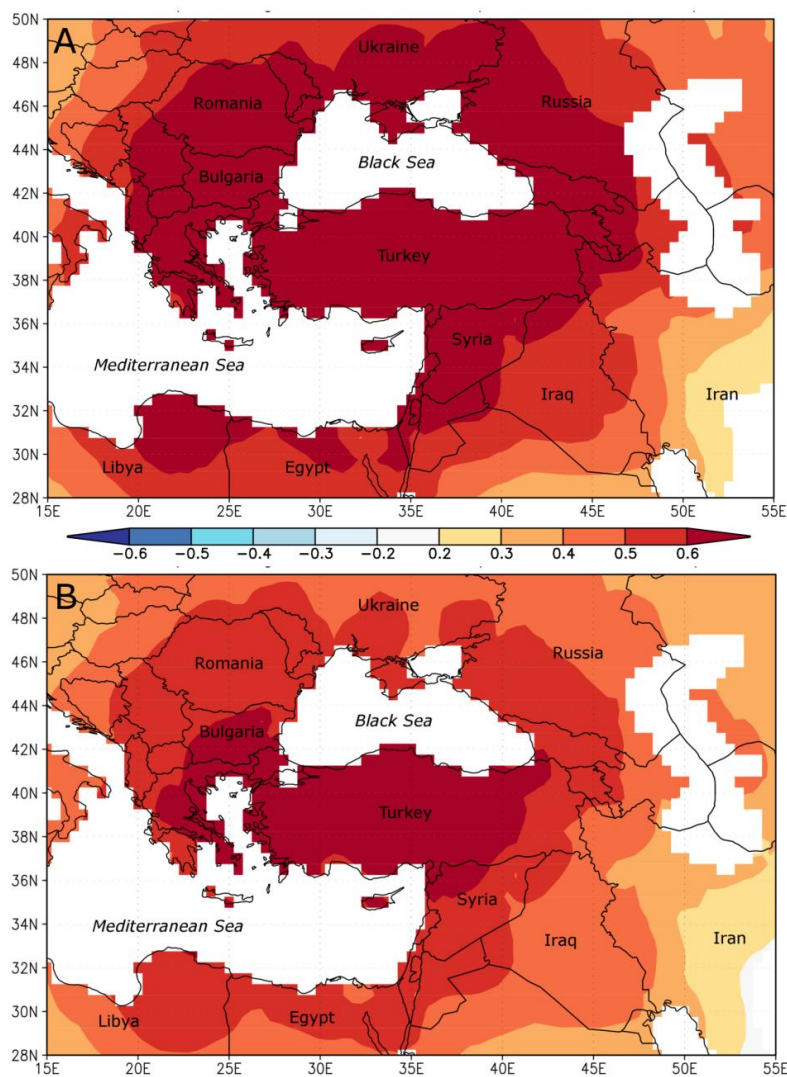
528 range 2–16 °C.

529

530

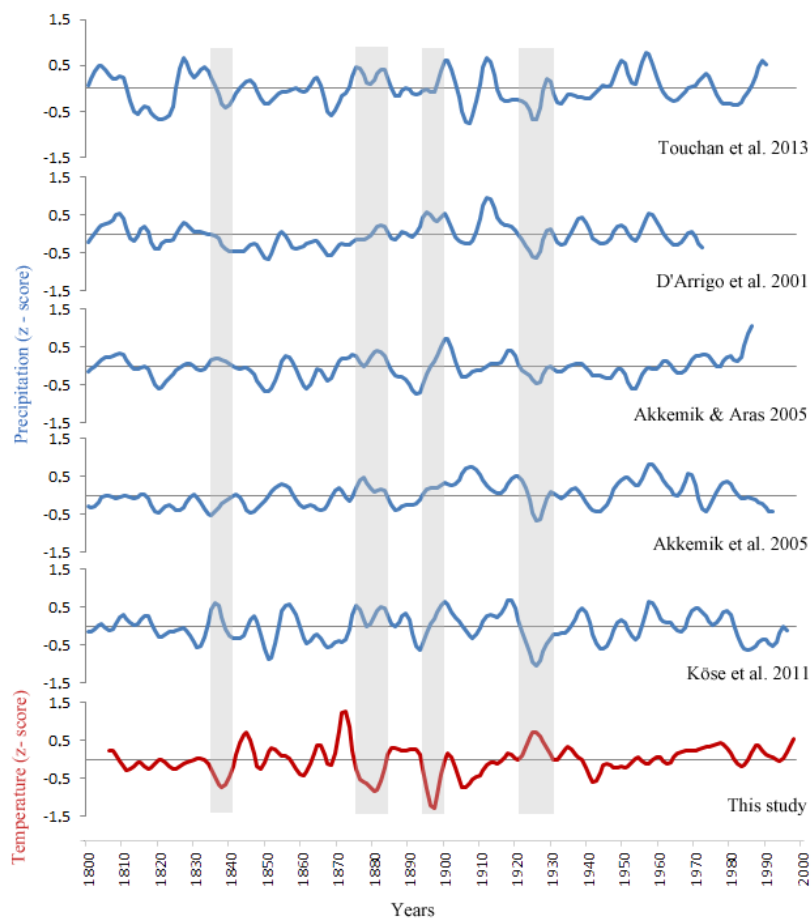
531

532



533

534 **Figure 6.** Spatial correlation map for the March–April temperature reconstruction. Spatial
535 field correlation map showing statistical relationship between the temperature
536 reconstruction and the gridded temperature field at 0.5° intervals (CRU TS3.23; Jones and
537 Harris 2008) during the period 1930–2002 [A] and 1901–1929 [B] over the Mediterranean
538 region.



539

540 **Figure 7.** Low-frequency variability of previous tree-ring based precipitation
541 reconstructions from Turkey and spring temperature reconstruction. Each line shows 13-
542 year low-pass filter values. z-scores were used for comparison.

543